Available online at www.sciencedirect.com
ScienceDirect
Journal of the European Ceramic Society 27 (2007) 4623–4631
www.elsevier.com/locate/jeurceramsoc

Effect of spinel content on slag attack resistance of high alumina refractory castables

L.A. Díaz [a], R. Torrecillas [a,*], A.H. de Aza [b], P. Pena [b]

[a] *Department of Chemistry of Materials, Instituto Nacional del Carbón-CSIC, C/Francisco Pintado Fe, 26, La Corredoria, 33011 Oviedo, Spain*
[b] *Instituto de Cerámica y Vidrio-CSIC, C/Kelsen, 5, Campus de Cantoblanco, 28049 Madrid, Spain*

Received 12 November 2006; received in revised form 9 April 2007; accepted 14 April 2007
Available online 27 June 2007

Abstract

High alumina refractory castables based on the Al_2O_3-MgO-CaO diagram ternary system were prepared using tabular alumina, white electrofused corundum, calcined alumina, synthetic spinel, dead-burned magnesia, dolomite, and calcium aluminate cement as starting raw materials. Two kinds of slags with 9.02 and 4.14 CaO/SiO_2 ratios were studied for slag resistance by means of crucible tests. The corrosion thickness increases with increase in magnesia content in all the designed compositions. The slag penetration decreases with increases in spinel content. Taking into account these results a refractory castable composition for its positioning into a steelmaking ladle was chosen.

Microstructural studies by SEM of samples taken from the slag line and wall in a steelmaking ladle were carried out. The correct amount of spinel required for practical applications was determined by the Al_2O_3-MgO-CaO-SiO_2 diagram quaternary system. A detailed model of the attack mechanisms is proposed.

Keywords: Alumina refractory castables; Spinel; Slag attack; Castables

1. Introduction

The rise of monolithic refractories has been a notable feature of the global refractory industry in recent years.[1] The development of castables for ladle linings has contributed to a rapid increase in the use of monolithic refractories in the field of iron and steel making. In the last two decades, Japanese authors[2,3] have reported the increasing use of Al_2O_3 spinel castables in secondary steel plants. Two factors have favoured their use:

(1) The growing tendency in the 1970s to replace magnesia-chrome bricks used in cement kilns by magnesia-spinel materials owing to waste disposal problems.
(2) In Japan in the period 1989–1991, the demand for cleaner steels, the unstable supply of zircon raw material, together with rising prices resulted in the development of new refractory linings. This represented a radical move away from ladle linings based on zircon and zircon-roseki castables to alumina-spinel castables.[4] The reduction in slag penetration and Mn^{2+}, Fe^{2+} and Fe^{3+} cations absorbed by the spinel in the form of a solid solution, were the key reasons for the improvement of the quality of alumina-spinel castables.[5]

There have been numerous studies on the effects of spinel on refractory castable properties, including the influence of spinel grain size,[6,7] chemical composition,[8] density,[9] spalling resistance[5] and hot strength.[10,11] Recently, the alumina-spinel castable normally used on the sidewall of secondary steelmaking ladles has gradually been replaced by an alumina-magnesia type.[12,13] The reason is that fine spinel formed "in situ" by the reaction of MgO-Al_2O_3 in the matrix of alumina-magnesia castables increases resistance to corrosion and slag penetration compared to alumina-spinel castables. However, there are several disadvantages to the use of magnesia. These include hydration problems, low workability, and a reduction in working time.[14–21]

Several authors have studied the corrosion of spinel-alumina castables. Nagai et al.[22] explain the slag wear mechanism in an alumina-spinel castable by means of the equiviscous-phase diagram of the CaO-SiO_2-FeO diagram ternary system. Mori

* Corresponding author.
E-mail addresses: ladiaz@incar.csic.es (L.A. Díaz), rtorre@incar.csic.es (R. Torrecillas).

0955-2219/$ – see front matter © 2007 Elsevier Ltd. All rights reserved.
doi:10.1016/j.jeurceramsoc.2007.04.007

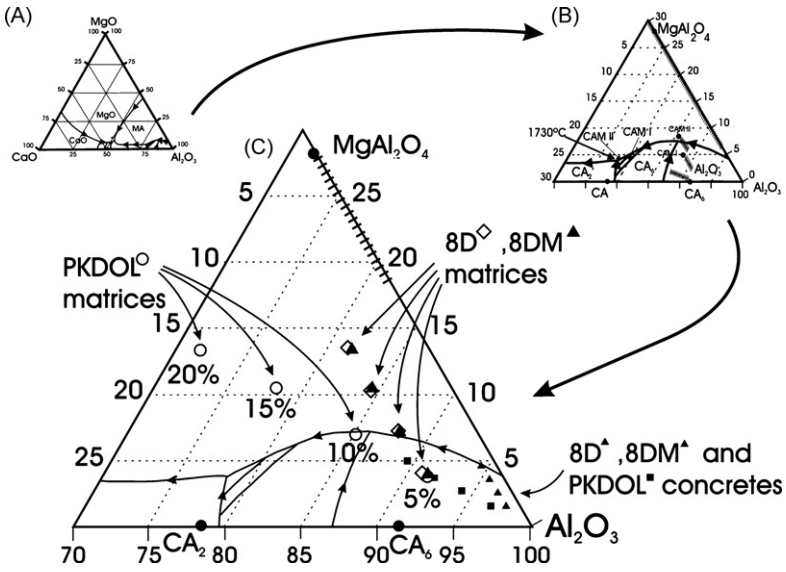

Fig. 1. (A) Al_2O_3-MgO-CaO ternary diagram system, (B) alumina-rich zone,[30] and (C) location of all the designed compositions in the alumina rich zone.

et al.[23] studied the behaviour of alumina-spinel castables for ladle lining with slags of various compositions. More recently, Korgul et al.[24] carried out a microstructural study on corroded alumina-spinel castable refractories, Sarpoolaky et al.[25] showed the influence of the grain phase on slag corrosion of low-cement castable refractories and Ko[26] examined the influence of the characteristics of spinels on resistance to slag attack in Al_2O_3-MgO and Al_2O_3-spinel castables. Minimum slag penetration in alumina-spinel castables occurs at spinel contents of around 20 wt%, slag penetration increasing with larger amounts of spinel.[22,27]

The purpose of the present work has been to explain the attack mechanisms of slags and molten steel on refractory castables elaborated according to the Al_2O_3-MgO-CaO system and the effect of the spinel content on the behaviour of the castables. The slag wear mechanisms were obtained on the basis of laboratory tests (crucible corrosion tests). The results obtained were used to select a refractory castable composition for a trial in an industrial secondary steel ladle.

2. Experimental procedure

Three kinds of refractory castables were elaborated in accordance with the Al_2O_3-MgO-CaO diagram ternary system. The following raw materials were used: tabular alumina (T-60),[b] white corundum,[c] calcined alumina (CT 9SG and CL 370C),[c] synthetic spinel,[c] periclase,[d] dolomite,[e] and calcium aluminate cement (CA 270).[c] The main differences between the elaborated concretes were in the composition of the matrix. The objective in their elaboration was that their matrices should have (fractions less to 125 μm) the same spinel content (5, 10, 15 and 20 wt%) on the basis of the following mixtures:

(1) Calcined alumina, synthetic spinel and calcium aluminate cement (8D compositions).
(2) Calcined alumina, magnesia and calcium aluminate cement (8DM compositions).
(3) Calcined alumina, dolomite and calcium aluminate cement (PKDOL compositions).

The procedure used to design and prepare the concretes has been explained in a previous publication.[28] Fig. 1 shows the location of all prepared compositions.

The castables for the crucible corrosion tests were cast in metal moulds and were cured at room temperature in airtight containers for 24 h and then dried at 110 °C for another 24 h before firing. All the specimens had the following dimensions: 110 mm × 110 mm × 80 mm with a diameter of 40 mm and holes 55 mm deep.

The laboratory crucible tests were performed independently with a fixed amount of slag (60 g) and steel (125 g) in each crucible. The castables were fired for 5 h at 1650 °C in a laboratory electric furnace and later crucibles were cross-sectioned perpendicular to their diameter. Crucible castable corrosion was evaluated on the basis of the loss of thickness from the original surface and penetration was defined as an attack via open porosity with or without chemical reaction. In Fig. 2A, a theoretical profile of the interior of the crucible before the slag attack (above) and after corrosion and penetration (below) is shown. By comparing the respective areas (before and after the attack) by computer analysis and normalizing the results, it was possible to evaluate the damage on each of the designed compositions. The open porosity of the designed castables at 1600 °C was studied following the UNE 61-033-90 Standard.

The slags were provided by two steel plants: EKO Stahl GmbH (Eisenhüttenstadt, Germany) and ARCELOR, S.A.

[b] Alcoa (Germany).
[c] Pechiney (France).
[d] Dead Sea Periclase (Israel).
[e] Prodomasa (Spain).

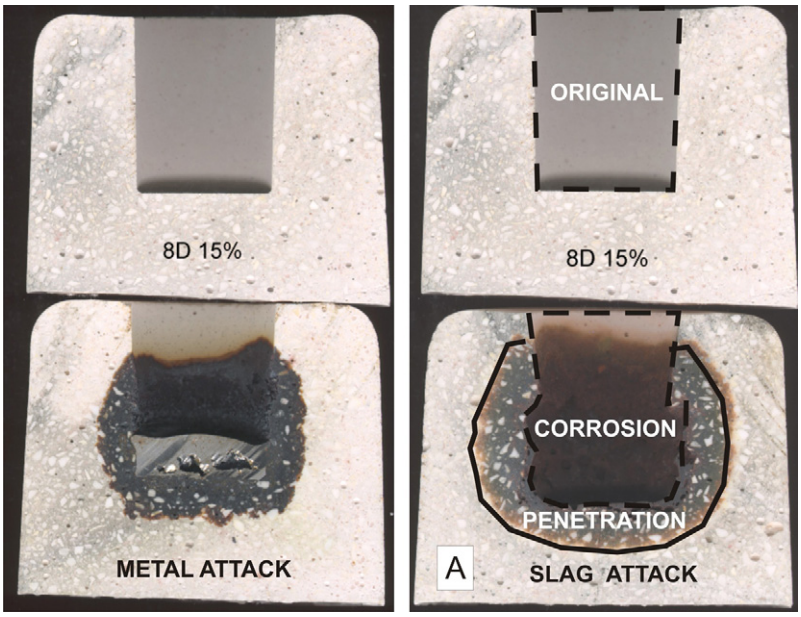

Fig. 2. Schematic diagram of the interior of the crucibles showing the extent of corrosion and penetration both metal as slag.

Table 1
Slag and steel chemical compositions supplied by EKO Stahl GmbH and ARCELOR (all values wt%)

Slag	Fe	FeO	SiO_2	CaO	MgO	Al_2O_3	MnO	P_2O_5	TiO_2	S
EKO	9.9	8.8	5.1	46	5.2	21	3.7	0.81	0.39	–
ARCELOR	12.1	15.6	13.4	55.5	6.9	1.1	4.1	1.2	0.50	0.69

Metal	C	Si	Mn	P	S	Al	Cr	Ni	Mo	Cu
EKO	0.032	0.007	0.208	0.007	0.006	0.038	0.016	0.027	0.002	0.027

(Gijón, Spain). In addition, EKO Stahl GmbH supplied the metal used in the crucible tests. The chemical compositions of the different slags and the metal were tested by XRF (Siemems SR-300) and the results are shown in Table 1. For X-ray diffraction (XRD), the samples were crushed and sieved (<40 μm) and the spectra recorded [over the range 2–65° (2θ)] on a Siemens D-5000 using Cu Kα radiation operating at 30 mA and 40 kV. Semi-quantitative phase contents were determined by reference to the integrated XRD peak intensities. In Table 2, the results obtained by XRD from the study of the slags are presented.

Table 2
Phase compositions and contents (semiquantitative) determined from XRD peak intensities of slags tested

Mineralogy	EKO slag	ARCELOR slag
Tricalcium aluminate, C_3A	***	
Mayenite, $C_{12}A_7$	**	*
Periclase, MgO	*	
Wustite, FeO	*	**
Lime, CaO	*	
Ca, Mn oxide	*	
Chrysotile, $Mg_3Si_2O_5(OH)_4$	*	*
Larnite, Ca_2SiO_4		***
Corundum, Al_2O_3		*
Calcite, $CaCO_3$		*
Ca,Fe oxide		*
Ca,Mn, silicate, $(Ca,Mn)_2SiO_4$		**

*** = High; ** = Medium; * = Low.

Guided by the crucible test results a refractory castable composition (8D10%) was chosen for an industrial trial in a secondary steel ladle from ARCELOR, S.A. The lining of the ladle used by this Company consist of two types of refractory brick materials: magnesia-carbon for the slag line and alumina refractory bricks with andalusite for the wall and bottom. The life span of the ladle was 295 castings, with continuous stops for maintenance (up to five) during which the evolution of thickness was controlled. Two types of samples were chosen (Fig. 3). The first tests were carried out on the slag line (A position, Fig. 3) (after 76 castings) and further tests were made on the wall (B position, Fig. 3) (295 castings), temporary shut-down of the ladle (to restore the refractory lining) was carried out. The samples were cut and impregnated with resin, ground and polished to 1 μm. Microstructural characterization of the samples, using secondary electron imaging and back-scattered electron imaging with the aid of a scanning electron microscope (SEM) (Zeiss, DSM 942-model) fitted with a Link Isis II energy-dispersive spectroscopy (EDS) analyser was performed.

3. Results and discussions

3.1. Laboratory tests

In Fig. 4, the effects of the attack by the EKO Stahl slag on all the designed compositions are shown. It should be pointed out

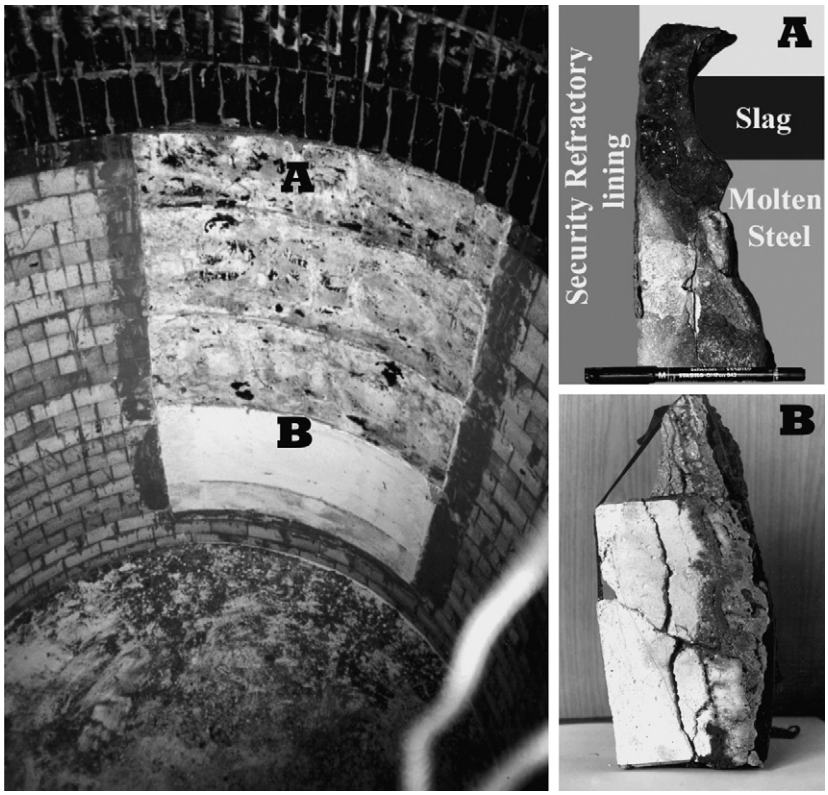

Fig. 3. An industrial trial in a secondary steel ladle from ARCELOR showing a window of 1.2 m × 2 m and the location of samples A (slag line) and B (wall) extracted.

that with an increase in synthetic spinel, magnesia or dolomite, corrosion increases slightly, while penetration by the molten slags decreases, except in the case of castables with dolomite, for which the extent of penetration is very similar in all cases. In other words, in the attack by the EKO Stahl slag with a $CaO/SiO_2 = 9.02$ ratio, corrosion and penetration show opposite trends as the amount of spinel or magnesia increases, while this divergence of trends is not observed for dolomite. On the other hand, compositions with magnesia present a slightly higher corrosion due to slag attack than those with synthetic spinel, while in the case of penetration (Fig. 4) the best behaviour corresponds to the magnesia compositions. This could be related: (1) the lower amount of open porosity present in the materials elaborated with magnesia (as opposed to spinel) at the temperature of around

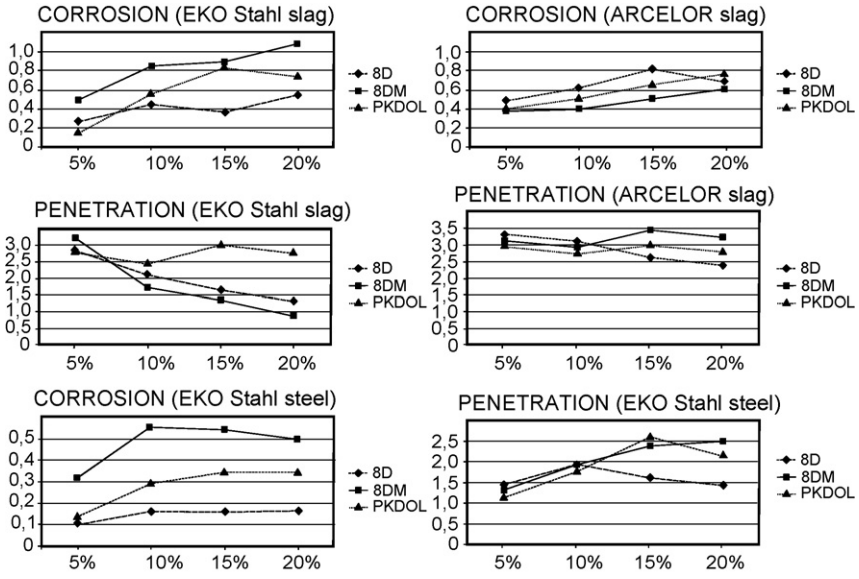

Fig. 4. Slag (EKO Stahl and ARCELOR) and metal (EKO Stahl) corrosion and penetration results for all the designed castables. The Y-axis represents the normalized transformed section in relation to the original hole size. Each point represents the average of three measurements.

1600 °C (Table 3), which would confirm the slightly greater densification of the matrix of the alumina-magnesia refractory castables due to the addition of periclase[29] and (2) changes in slag composition due to the slag reacting with the refractory microstructure. Thus, CaO reacts with the alumina to form CA_2 and CA_6, while Mn^{2+}, Fe^{2+} and Fe^{3+} cations are absorbed by spinel to form a solid solution. The residual molten liquid becomes rich in SiO_2 and increases its viscosity. Furthermore, the temperature inside the refractory castable decreases following a characteristic temperature distribution and penetration is suppressed.[22]

The castables behaviour changed when using the slag provided by ARCELOR (Fig. 4). In this case, for the corrosion tests, a CaO/SiO_2 slag ratio = 4.14 was added to the crucibles. The level of corrosion increased from 5 to 20% for the raw materials added (spinel, periclase, and dolomite). With this kind of slag, 8D type castables present higher levels of corrosion than the 8DM ones. Regarding penetration, the results are more or less homogeneous, with no significant differences between the designed compositions. Only in the case of the 15 and 20% compositions, very small slag penetration changes were observed.

Concerning the molten steel from EKO Stahl, the comparative behaviour in the corrosion and penetration tests for the three types of compositions is shown in Fig. 4.

The obtained results show that the degree of corrosion for steel is slightly higher in the 8DM type compositions compared to the rest, while in the case of penetration of the steel, the 8D compositions show a better behaviour.

Taking into account the physical properties of the elaborated refractory castables and the laboratory crucible test results the 8D 10% composition was chosen for an industrial trial into a secondary steel ladle.

3.2. Industrial trial

3.2.1. Samples from the slag line

Fig. 3 (photograph A) shows a view of the final state of the 8D10% refractory concrete at the slag line of the secondary steel ladle from ARCELOR after 76 castings. Significant erosion can be observed at the triple junction (refractory-molten liquid-air). This work area is subject to permanent erosion due to the continuous change in slag composition (fresh-slag). A cross-section of the microstructure obtained by SEM at low magnification is shown in Fig. 5. The penetration area is confined to a thickness of about 15 mm and is formed by a first layer of metallic magnesium of about 2 mm thickness containing glass rich in magnesia. This layer is encrusted and does not derive from the slag attack on the refractory castable. Under this layer, there is a dense spinel layer with solid solutions of Fe and Mn, as well as hercynite ($Fe_2Al_2O_4$) white contrast in the micrograph and shows a texture indicative of fluid flow. In this area no alumina crystals can be observed. The thickness of this spinel layer is about 400–500 μm. Immediately under this layer, there is a dual microstructure formed by large alumina grains several millimetres wide (tabular alumina) as well as electrofused rounded corundum grains ~200 μm thick. Both grain types are surrounded by a dense matrix formed by three phases: CA_6 crystals in the form of elongated plates, isolated spinel crystals and a matrix of anorthite ($CaAl_2Si_2O_8$) needles. This area of the refractory castable is characterized by a completely reacted matrix (except in the case of the spinel crystals) which still retains the structure and composition of the largest grains such as alumina.

The attack mechanism of the refractory concrete against the molten slag can be explained with the help of the Al_2O_3-MgO-CaO-SiO_2 quaternary diagram. Although in this system there are many compatibility tetrahedrons where the spinel phase is present, Fig. 6 shows in a simplified form those tetrahedrons which are projected onto the CaO-SiO_2-Al_2O_3 composition tetrahedron. At this point several factors need to be considered. First it is important to distinguish between the composition of the matrix and the concrete. The 8D10% concrete composition is located inside the primary crystallization field of the alumina, while the one of the matrix is located in the spinel area (see Fig. 1). Both, the concrete and the matrix, are located in the Al_2O_3-$MgAl_2O_4$-$CaAl_2Si_2O_8$-$CaAl_{12}O_{19}$ compatibility tetrahedron presenting a fixed invariant point at 1400 °C. Fig. 6 shows the Al_2O_3-MgO-CaO-SiO_2 quaternary diagram in which some of the eutectic binary surfaces defining the primary crystallization field of the spinel are represented, as well as the isothermal plane at 1650 °C (working temperature of the refractory castable in contact with the slag). Three hypothetical slag compositions with different CaO/SiO_2 ratios are shown on the quaternary diagram. Slag 1 corresponds to the ARCELOR slag. Its attack process is as follows: when slag 1 melted at 1650 °C is in contact with the 8D10% refractory castable, the finest fractions of the refractory (matrix) dissolve. In this way, the glassy phase formed at the interface moves its composition along the line that links the matrix composition and the slag. When the composition reaches point 1, being located on the isothermal plane at 1650 °C, the spinel present in the matrix stops dissolving. However, the other phases continue to dissolve and move their composition along the line formed by the intersection of the isothermal plane and the plane that contains the spinel composition, the matrix and slag 1. A dense spinel layer is then formed. This layer absorbs metallic cations such as Fe^{2+}, Fe^{3+} and Mn^{2+} as a solid solution. The melted solution penetrates through the matrix which is also dissolved. Likewise, the surfaces of the largest grains are also attacked, as can be observed in Fig. 5. When the melted solution reaches the composition at point A, being located on the eutectic binary surface that separates the primary fields of CA_2 and the spinel, CA_2 precipitates from the glass. The solution moves its composition along the intersection line that separates the isothermal plane from the eutectic binary surface (now rich in SiO_2) up to point X. At this point CA_6 precipitates and the glass becomes poor in alumina and CaO and rich in SiO_2. Due to the position of the isothermal plane during the precipitation of CA_6, the glassy phase is reduced while its viscosity is increased. The composition of the glass continues to change until it reaches point Y, a composition being in equilibrium with all the phases present in the refractory. Consequently, at 1650 °C, the glass with a composition of Y, spinel and CA_6, originating from

Table 3
Open porosity results of the castables fired at 1600 °C

Temperature	8D open porosity (%)				8DM open porosity (%)				PKDOL open porosity (%)			
	5	10	15	20	5	10	15	20	5	10	15	20
1600 °C	22.53	22.45	22.23	21.64	22.74	21.52	21.02	19.73	22.65	24.80	26.79	28.48

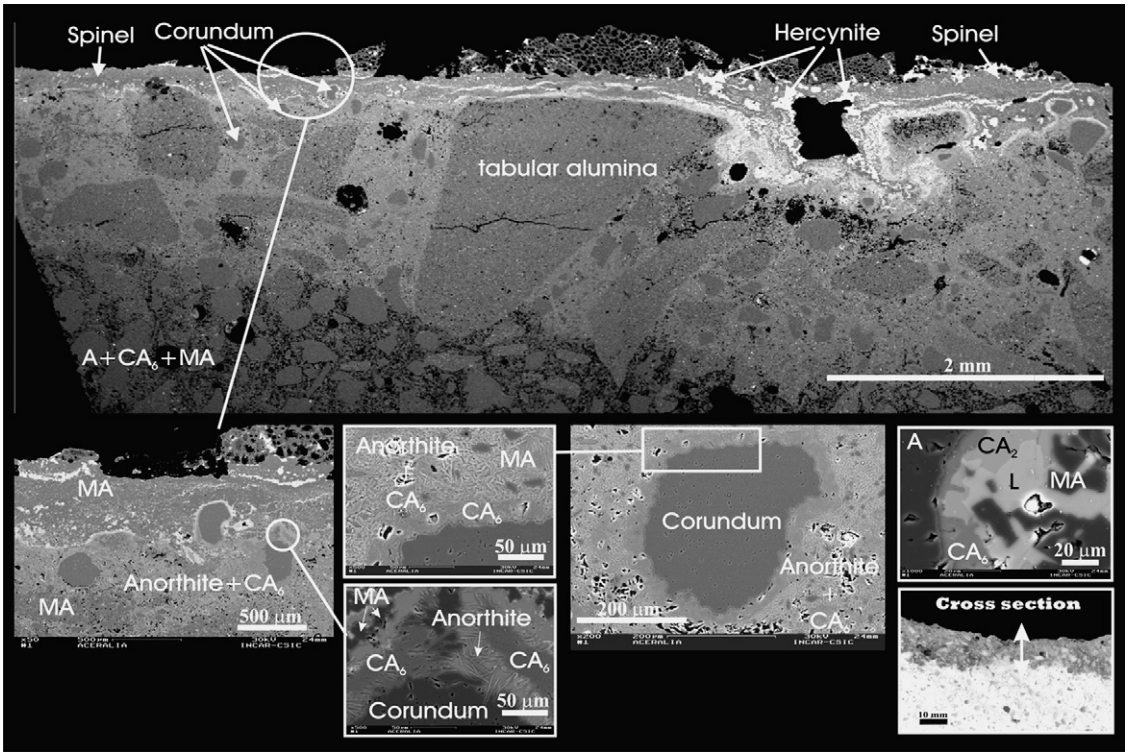

Fig. 5. Microstructures by SEM of a cross-section from the sample extracted at the slag line (zone A, see Fig. 3).

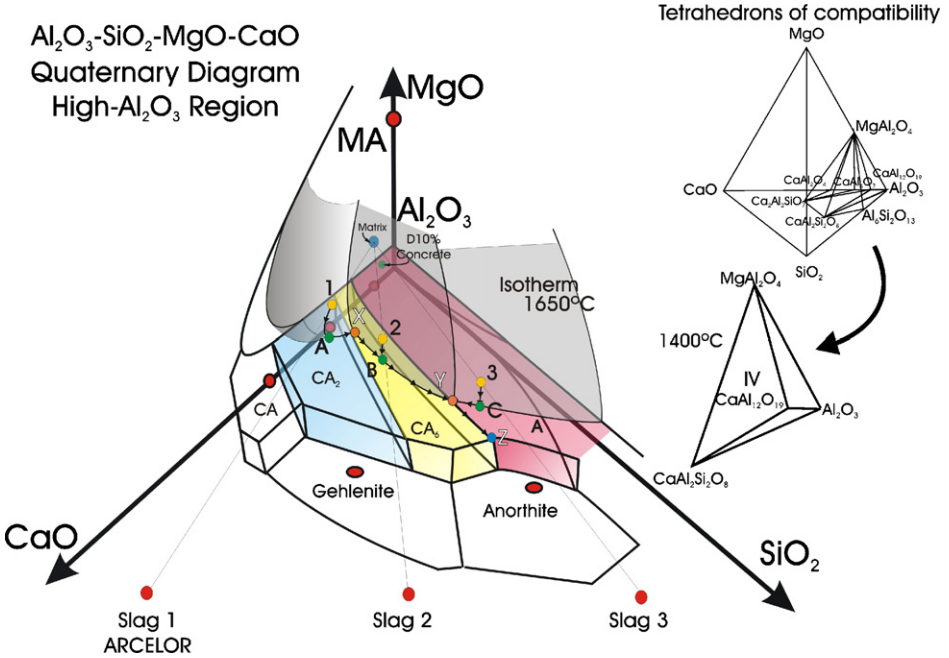

Fig. 6. Graphical representation of the attack mechanism of the refractory concrete against molten slag from ARCELOR using the Al_2O_3-MgO-CaO-SiO_2 quaternary diagram.

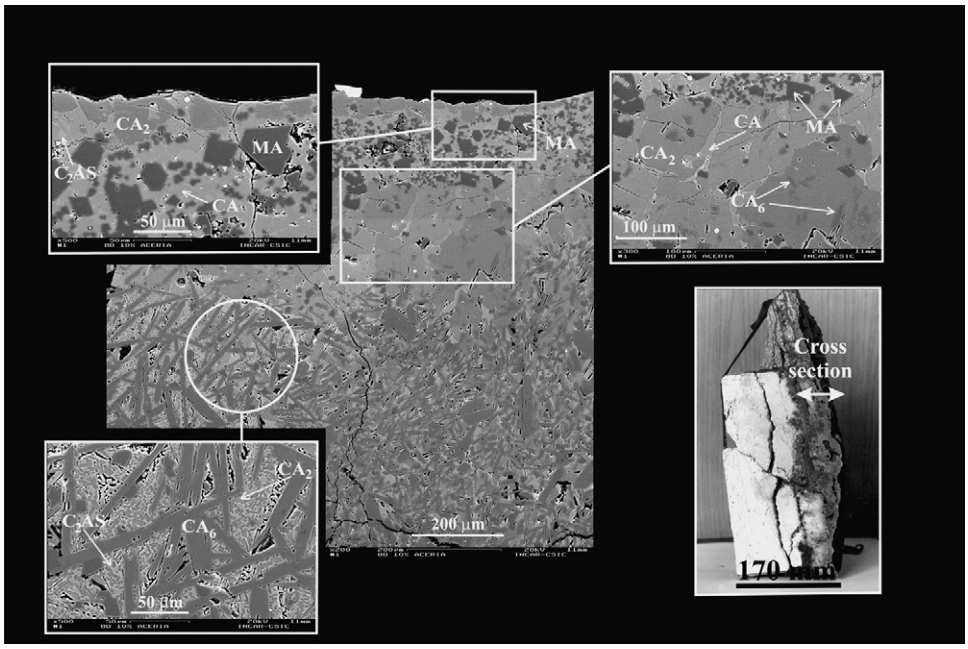

Fig. 7. Microstructures by SEM of a cross-section from the sample extracted at the wall (zone B, see Fig. 3).

the reaction of the calcium aluminate cement with the alumina present in the refractory and the largest alumina grains that have only partially been attacked, are probably in equilibrium. During cooling, the glass composition moves along the eutectic ternary line that separates the CA_6, alumina and spinel primary fields of crystallization, until it reaches the invariant point located at 1400 °C (point Z). At this point, anorthite crystallization takes place and the vitreous phase disappears.

3.2.2. *Samples from the wall*

During the shut-down of the ladle, a sample was extracted from that part of the wall which was in contact with the andalusite lining (Fig. 3, B point) and subjected to XRD and SEM analysis. The evolution of the phases is similar to that found on the slag line with slight differences which will be discussed later. In this case the refractory castable presents a layer of attached slag several millimetres thick, which was not found on the slag line due to the presence of convection currents that dispersed the melted phases over the surface of the refractory. Fig. 7 shows some of the salient features revealed by SEM. Several areas can be observed:

(1) At the surface, CA_2 crystals are apparent.
(2) A layer about 200 μm thick formed by two types of spinel crystals surrounded by a glassy phase. Small crystals, some 10 μm wide and larger crystals of 50 μm, are also present. The latter exhibit Mn^{2+} and Fe^{2+} in solid solution in greater proportions than in the 10 μm crystals.
(3) A zone about 250–300 μm wide, consisting of large CA_2 crystals and CA_6 precipitates. These microcrystals have grown inside their primary crystallization field.
(4) At about 500 μm below the surface, two different microstructures appear in separate areas, representing clearly differentiated regions: (a) in one of these areas, primary CA_6 crystals with a high aspect ratio and an acicular shape can be observed. Among these, there are isolated spinel crystals, and CA_2 crystals surrounded by a gehlenite matrix (C_2AS). (b) In other areas, a matrix of CA_6 crystals surrounded by a gehlenite matrix can be seen.
(5) In the area which has not been attacked (Fig. 8), tabular alumina grains and large corundum crystals appear to have partially reacted with the matrix forming a dense layer of CA_6 having grown through the alumina crystals. In this area, the matrix is formed by both CA_6 platelets and spinel. This complex microstructure can be attributed to the heterogeneous composition of the refractory. The kinetics of the attack process on both, the matrix and the rough particles, is different in each case. In the present study, the white electrofused corundum is more resistant to slag corrosion than the alumina tabular grains.[25] In this microstructure there are no large alumina grains on the attacked surface as there are on the slag line. This may be due to the fact that they have had time to dissolve through a layer being at least several millimetres thick. This is significant since it implies that the composition that we should be considering is the global composition of the refractory.

If we look at Fig. 9, in which the isothermal plane (at 1650 °C) of the Al_2O_3-MgO-CaO ternary diagram system is represented, it can be observed that when the composition of the slag is linked with the refractory castable composition, the line intercepts the stability field of the CA_2 + liquid (point C in Fig. 9) instead of MA + liquid (point A in Fig. 9). This means that on the surface the CA_6 and spinel crystals are not stable phases. CA_2 is the stable phase, which explains the precipitation of a thick layer of CA_2 in the microstructure. The dissolution process of the spinel concludes when point B is reached (Fig. 9). At this point,

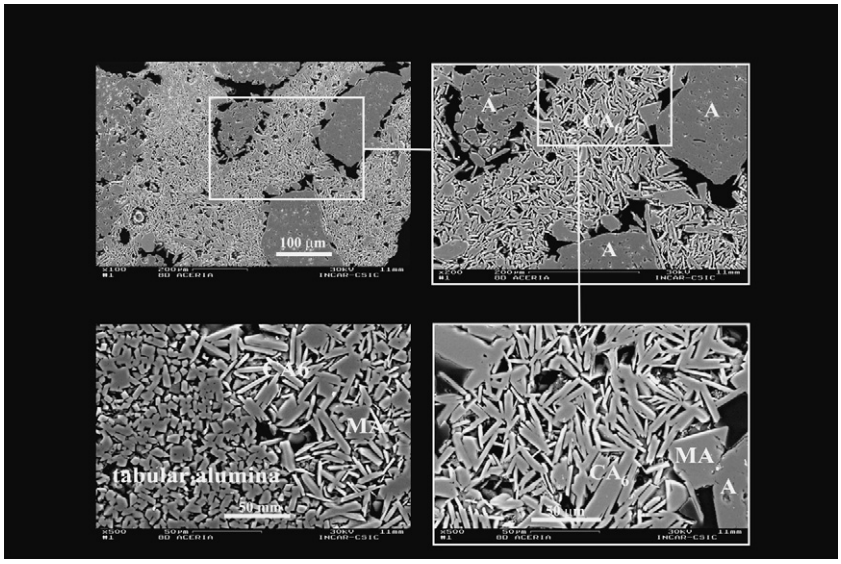

Fig. 8. Microstructures by SEM of a cross-section from the sample far from the attacked area. A (alumina), MA (spinel).

the spinel crystals, CA_2 and a glass with composition B are possibly in equilibrium. To better understand the attack it is again necessary to examine the quaternary diagram in Fig. 6. Point A on the quaternary diagram (Fig. 6) is identical to point B on the ternary (Fig. 9). The glass changes its composition along the intersection of the isothermal plane and the eutectic binary plane until it reaches point X (Fig. 6). At this point CA_6 precipitates, as can be observed in the micrographs of Fig. 7. Due to the thick layer of CA_2, the temperature rapidly decreases inside the refractory castable, with gehlenite (C_2AS) precipitating from the melted glass as it cools instead of anorthite (CAS_2), as occurred in the case of the materials located at the triple junction of the ladle. For such good slag resistence behaviour in this type of refractory, it is essential for the spinel to be the first stable phase. Hereby two parameters play an important role here: the slag composition and the matrix composition of the refractory. Slags with a high magnesium content will cause the intersection point on the liquidus lines to occur above the calcium aluminates field (see Fig. 9). Similarly, a matrix of the refractory castable with a high MgO content will have the same effect.[13]

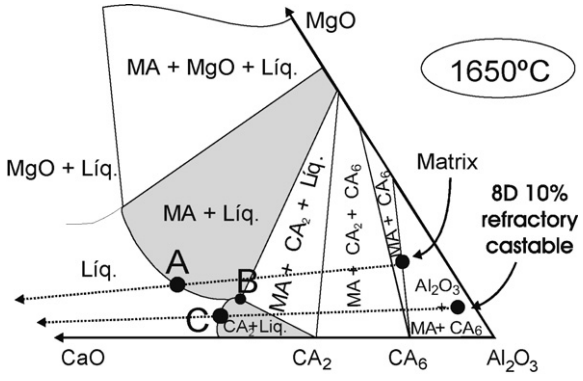

Fig. 9. Isothermal plane at 1650 °C of the Al_2O_3-MgO-CaO ternary diagram system showing the reaction path of ARCELOR slag against both the matrix and the 8D10% concrete.

4. Conclusions

The present study shows that by means of the Al_2O_3-MgO-CaO-SiO_2 diagram quaternary system slag penetration of the designed refractory castables is reduced due to the presence of alumina and spinel (whether synthetic or self-forming) in their matrices, while the CaO, FeO and MnO oxide components of the slag are captured. As a result, the composition of the slag changes, becoming rich in SiO_2, and more viscous causing the penetration to stop altogether.

Resistance to corrosion and slag attack by high alumina refractory castables depends on the composition of the slag and the kind of refractory used. Laboratory crucible tests showed: (1) corrosion thickness increases with the increase in magnesia content in all the designed compositions (type 8D, 8DM and PKDOL), (2) slag penetration (EKO Sthal slag with C/S = 9) decreases from 5 to 20% spinel content for the 8D and 8DM compositions, while for penetration with C/S = 4 (ARCELOR slag) there is also a slight decrease, although mainly regarding the 15 and 20% 8D and 8DM compositions.

SEM shows that samples taken from the slag line and the wall of the steelmaking ladle possess two different microstructures. The slag line is subject to permanent erosion and the refractory castable being in contact with the melted slag forms a layer of 400–500 μm of spinel crystals and several thick layers of hercynite indicative of fluid flow. Immediately under these layers are large (μm) alumina grains (tabular alumina and white electrofused corundum) inside a dense matrix formed by: CA_6 crystals, spinel crystals and anorthite needles. By contrast, the microstructure observed in samples of the wall shows CA_2 crystals in contact with the slag. Next, a 200 μm thick layer is formed by spinel grains and then more CA_2 crystals appear together CA_6 and gehlenite crystals.

The amount of spinel required to ensure maximum performance can be calculated using the Al_2O_3-MgO-CaO-SiO_2 diagram quaternary system. Fundamentally, it is also neces-

sary that the spinel be a stable phase even in contact with the melted solution. However, slags with a high magnesium content or matrices of the castables with high MgO content will also favour resistance to penetration.

Acknowledgments

The authors wish to thank the European Union for its support under a Brite Euram Project (Contract No. BRPR-CT 97-0427). Also thanks to the anonymous referee of this paper for their constructive suggestions.

References

1. Kendall, T., Steel industry monolithic: Castables setting the pace. *Ind. Miner.*, 1995, 33–45.
2. Nagai, B., Matsumoto, O. and Isobe, T., Development of monolithic refractory lining for BOF ladle in Japan mainly for the last decade. In *Proceedings of UNITECRĭ91 Congress*, 1991, pp. 83–86.
3. Isobe, T., Matsumoto, O., Itose, S., Kawano, F., Saihi, K., Takiuchi, S. and Oda, Y., Sinterability of spinel raw fine powder and application to castables. *Taikabutsu Overseas*, 1995, **15**(3), 10–13.
4. Kataoka, S., Refractories for steelmaking in Japan. In *Proceedings of UNITECRĭ95 Congress*, 1995, pp. 1–27.
5. Sumimura, S., Yamamura, T., Cubata, Y. and Kanashige, T., Study on slag penetration of alumina-spinel castable. In *Proceedings of UNITECRĭ93, Sao Paulo, Brazil*, 1993, pp. 97–101.
6. Ohish, I. and Ebizawa, R., Application of alumina–spinel castable refractories to steel ladle. In *Proceedings of UNITECRĭ91 Congress*, 1991, pp. 101–107.
7. Nakashima, M., Isobe, T., Itose, S., Touno, A. and Shimizu, I., Improving the Corrosion Resistance of Alumina-Spinel Castable by Adding Ultrafine Spinel. In *Taikabutsu Overseas, Abstracts of the 10th Annual Colloquium of TARJ, Vol 17, no. 4*, 1997, p. 96.
8. Mori, J., Onove, M., Toritani, Y. and Tanaka, S., Structure change of alumina castable by addition of magnesia or spinel. *Taikabutsu Overseas*, 1995, **15**(3), 20–23.
9. Sato, Y., Joguchi, H. and Hiroki, N., Test results of alumina-spinel castables for steel ladle. *Taikabutsu Overseas*, 1992, **12**(3), 10–14.
10. Ko, Y. C. and Chan, C. F., Effect of spinel content on hot strength of alumina-spinel castables in the temperature range 1000–1500 °C. *J. Eur. Ceram. Soc.*, 1999, **19**, 2633–2639.
11. Chan, C. F. and Ko, Y. C., Effect of CaO content on the hot strength of alumina-spinel castables in the temperature range 1000–1500 °C. *J. Am. Ceram. Soc.*, 1998, **81**(11), 2957–2960.
12. Nakashima, M., Isobe, T., Itose, S., Touno, A. and Shimizu, I., Improving the corrosion resistance of alumina-spinel castable by spinel additions. *J. Techn. Assoc. Refract. Jpn.*, 2001, **21**(3), 155–161.
13. Ko, Y. C., Influence of the characteristics of spinels on the slag resistance of Al_2O_3-MgO and Al_2O_3-spinel castables. *J. Am. Ceram. Soc.*, 2000, **83**(9), 2333–2335.
14. Shima, K., Imaiida, Y. and Katani, T., Application of alumina-spinel castable to teeming ladle for stainless steel. *Taikabutsu Overseas*, 1995, **15**(3), 24–28.
15. Brandao, P., Goncalves, G. E. and Duarte, A. K., Mechanisms of hydration/carbonation of basic refractories. *Refract. Appl.*, 1998, **3**(2), 6–8.
16. Brandao, P., Goncalves, G. E. and Duarte, A. K., Mechanisms of hydration/carbonation of basic refractories. PT.2. Investigation of the kinetics of formation of brucite in fired basic bricks. *Refract. Appl.*, 1998, **3**(2), 9–11.
17. Kaneyasu, A., Yamamoto, S. and Yoshida, A., Magnesia raw materials with improved hydration resistance. *Taikabutsu Overseas*, 1997, **17**(2), 21–26.
18. Kaneyasu, A., Arita, Y., Yoshida, A. and Watanabe, T., Hydration resistance of MgO aggregate with added CaO. *Taikabutsu Overseas*, 1999, **19**(1), 30–34.
19. Kaneyasu, A., Yamamoto, S. and Watanabe, T., MgO raw material with improved hydration resistance. *Taikabutsu Overseas*, 1996, **16**(2), 26–30.
20. Kitamura, A., Onizuka, K. and Tanaka, K., Hydration characteristics of magnesia. *Taikabutsu Overseas*, 1996, **16**(3), 3–11.
21. Lee, W. E., Vieira, W., Zhang, S., Ghanbari Ahari, K., Sarpoolaky, H. and Parr, C., Castable refractory concretes. *Int. Mater. Rev.*, 2001, **46**, 145–167.
22. Nagai, B., Matsumoto, O., Isobe, T. and Nishiumi, Y., Wear mechanism of castable for steel ladle by slag. *Taikabutsu Overseas*, 1992, **12**(1), 15–20.
23. Mori, J., Yoshimura, M., Oguchi, Y., Kawakami, T. and Ohishi, I., Effect of slag composition on wear of alumina-spinel castable for steel ladle. *Taikabutsu Overseas*, 1992, **12**(1), 40–45.
24. Korgul, P., Wilson, D. R. and Lee, W. E., Microstructural analysis of corroded alumina-spinel castable refractories. *J. Eur. Ceram. Soc.*, 1997, **17**, 77–84.
25. Sarpoolaky, H., Zhang, S., Argent, B. B. and Lee, W. E., Influence of grain phase on slag corrosion of low-cement castable refractories. *J. Am. Ceram. Soc.*, 2001, **84**(2), 426–434.
26. Ko, Y.-C., Influence of the characteristics of spinels on the slag resistance of Al_2O_3-MgO and Al_2O_3-spinel castables. *J. Am. Ceram. Soc.*, 2000, **83**(9), 2333–2335.
27. Oguchi, Y. and Mori, J., Wear mechanism of castable for steel ladle. *Taikabutsu Overseas*, 1996, **13**(3), 43–49.
28. Diaz, L. A., Torrecillas, R., De Aza, A. H., Pena, P. and De Aza, S., Alumina-rich refractory concretes with addded spinel, periclase and dolomite: A comparative study of their microstructural evolution with temperature. *J. Eur. Ceram. Soc.*, 2005, **25**(9), 1499–1505.
29. Kobayashi, M., Kataoka, K., Sakamoto, Y. and Kifune, I., Use of alumina-magnesia castables in steel ladle sidewalls. *Taikabutsu Overseas*, 1997, **17**(3), 39–44.
30. De Aza, A. H., Pena, P. and De Aza, S., The System Al_2O_3-MgO-CaO. Part I. Primary phase field in the subsystem $MgAl_2O_4$-$CaAl_4O_7$-CaO-MgO. *J. Am. Ceram. Soc.*, 1999, **82**(8), 2193–2203.